Herschel characterization of evolved HII regions in the Hi-GAL SDP field at l= 30^0

Roberta Paladini
(IPAC/ California Institute of Technology)

Co-authors: G. Umana, L. D. Anderson, M. Veneziani, A. Noriega-Crespo, D. Paradis, F. Piacentini, J.-P. Bernard, P. Natoli

ESLAB 2010 – May 6th, Nordwjik, Netherlands

Credit: Hi-GAL Cosortium

OUTLINE OF THE TALK

- ✓ The Hi-GAL survey
- ✓ Evolved HII regions: the context
- ✓ Building FIR/sub-mm SEDs
- ✓ The β - T relation
- ✓ Color - color plots
- ✓ Conclusions

The Herschel infrared Galactic Plane Survey: Hi-GAL (P.-I.: S. Molinari)

o Hi-GAL is observing the first and fourth Galactic quadrant using the PACS and SPIRE instruments in parallele mode.

o During the SDP, two Hi-GAL fields ($2^0 \times 2^0$) have been observed. The fields are centered at l = 30^0 and l = 59^0 (|b| < 1^0).

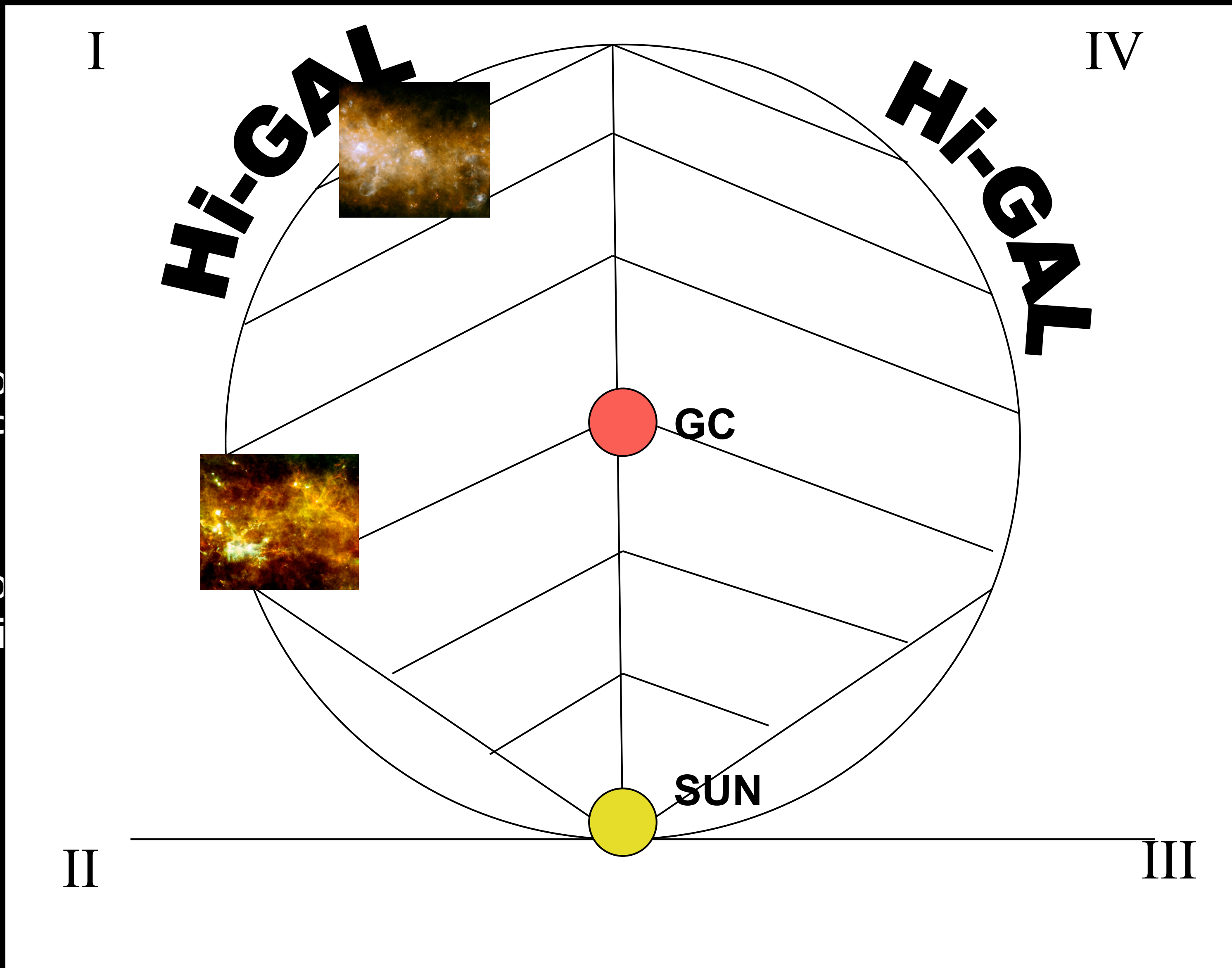
I
IV
Hi-GAL
Hi-GAL
GC
SUN
II
III

Evolved HII regions: context

- HII regions are sites of ionized gas surrounding associations of OB stars.
- They correspond to a late stage of the massive star formation process, during which stars are not only formed but also on the main sequence.
- The evolutionary sequence of HII regions spans different phases, with each phase being characterized by typical values of electron density, n_e, and linear diameter, d, (Kurtz 2005):

✓ Hyper-compact HII regions (HCHII): $n_e > 10^6$ cm^{-3}, d < 0.05 pc, radio loud but optically thick spectrum up to several GHz, broad (> 40 Km/sec) RRL, no clear-cut evidence for dust emission ;

✓ Ultra-compact / compact HII regions (UCHII): $n_e \sim 10^3 - 10^4$ cm^{-3} , d ~ < 0.1 - 0.5 pc, radio loud and optically thick spectrum up to several GHz, narrower RRL (< 40 Km/sec), intense associated dust emission;

✓ Evolved HII regions: $n_e \sim 10^2$ cm^{-3}, d ~ a few pc, radio loud and optically thin > ~ 1 GHz, , narrow RRL (< 40 Km/sec), dust emission, optically visible (if close enough, i.e. < ~ 1 -2 kpc)

The use of ancillary single-dish radio data:

1. Definition of the sample

- We use the reference radio catalog of Paladini et al. (2003). While for $29^0 < l < 31^0$, $|b| < 1^0$, the catalog lists 30 HII regions, for $58^0 < l < 61^0$, $|b| < 1^0$, we have only two sources. Therefore we focus our analysis on the SDP field centered at $l = 30^0$.

- We cross-check the source selection from Paladini et al. (2003) with SIMBAD.

- Out of the 30 cataloged sources, we choose only the objects for which ancillary information is available, in particular those for which an estimate of the distance can be derived (cfr. Anderson & Bania, 2009). This further selection leaves us with 17 sources. For these, we compute T_e, EM and n_e according to:

1) $$T_e[K] = (372 \pm 38) R_G + (4260 \pm 350)$$ (Deharveng et al., 2000)

2) $$T_b = 8.235 \times 10^{-2} a \left(\frac{T_e}{K}\right)^{-0.35} \left(\frac{\nu}{GHz}\right)^{-2.1} \int n_e^{\,2} ds$$ (Mezger & Henderson, 1967)

3) $$< n_e > = \frac{\sqrt{EM}}{d}$$

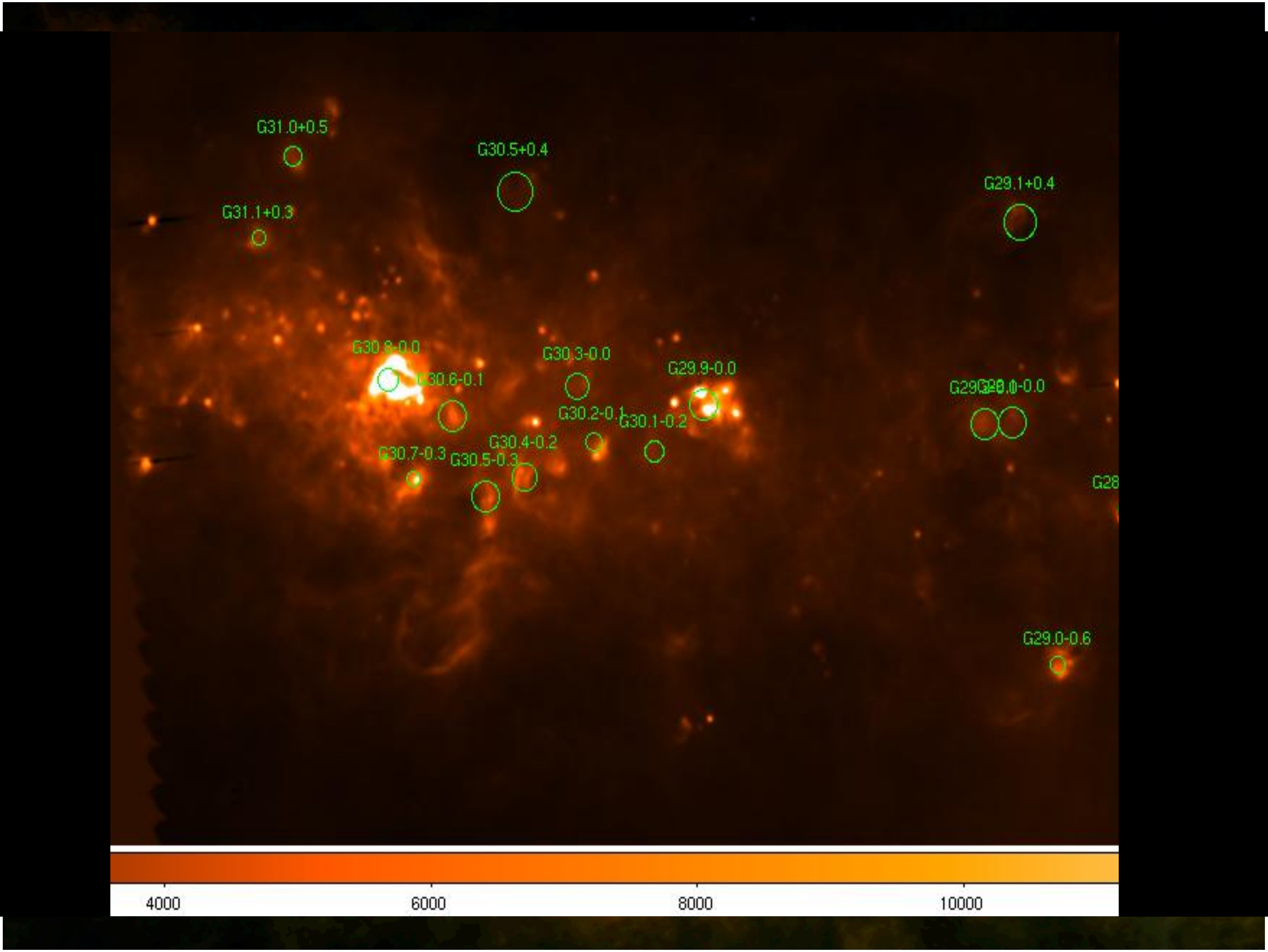
G31.0+0.5
G30.5+0.4
G29.1+0.4
G31.1+0.3
G30.8-0.0
G30.3-0.0
G29.9-0.0
G30.6-0.1
G30.2-0.1
G30.1-0.2
G30.4-0.2
G30.7-0.3
G30.5-0.3
G29.0-0.6
4000
6000
8000
10000

SELECTED SAMPLE

Name	l (deg)	b (deg)	S (Jy)	diam (arcmin)	R (kpc)	D (kpc)	V_{LSR} (km/s)	T_e (K)	d (pc)	EM ($pc*cm^{-6}$)	n_e (cm^{-3})
G28.8-0.2	28.823	-0.226	1.47	2.2	4.5	5.5	90.6	5934	3.5	8.2e4	152.7
G29.0-0.6	28.983	-0.603	1.01	2.3	5.8	11.5	52.6	6417	7.7	5.3e4	83.0
G29.1-0.0	29.136	-0.042	1.85	4.3	5.8	11.5	52.4	6417	14.4	2.7e4	43.9
G29.1+0.4	29.139	0.431	2.68	4.8	7.4	13.6	21.9	7012	19.0	3.3e4	41.8
G29.2-0.0	29.205	-0.047	2.22	4.3	5.4	10.9	61.7	6268	13.6	3e3e4	49.2
G29.9-0.0	29.944	-0.042	16.64	4.3/6.6	4.5	6.0	97.8	6510	11.5	1.1e5	92.8
G30.1-0.2	30.069	-0.160	0.95	3.0	4.4	8.5	98.2	5897	7.4	2.8e4	61.9
G30.2-0.1	30.227	-0.145	2.59	2.6	4.4	7.8/9.5	99.0	9100	5.8/7.2	1.2e5	142.7/129.4
G30.3-0.0	30.277	-0.020	0.73	2.8	4.4	6.2	97.9	5896	5.0	2.5e4	70.5
G30.4-0.2	30.404	-0.238	3.59	3.7	4.3	8.0	102.5	5959	8.6	7.0e4	90.5
G30.5-0.3	30.502	-0.290	2.96	4.3	4.3	7.3	107.3	5860	9.1	4.3e4	68.7
G30.5+0.4	30.467	0.429	2.13	5.4	5.2	3.6/10.1	57.7	6194	5.7/15.9	2.0e4	59.5/35.5
G30.6-0.1	30.602	-0.106	2.40	2.3	4.4	7.3	102.5	6800	4.9	1.3e5	162.2
G30.7-0.3	30.694	-0.261	3.27	2.2	4.5	8.3	98.5	6800	5.3	1.9e5	189.9
G30.8-0.0	30.776	-0.029	62.17	3.2/6.2	4.6	5.7	91.6	7030	5.3	4.6e5	193.3
G31.0+0.5	31.050	0.480	1.75	2.8	7.1	12.9	27.9	6901	10.5	6.3e4	77.8
G31.1+0.3	31.130	0.284	1.11	2.0	4.4	7.3	104.7	5896	4.2	7.4e4	132.0

SELECTED SAMPLE

Name	
G28.8	7
G29.0	0
G29.1	
G29.1	
G29.2	.2
G29.9	8
G30.1	
G30.2	29.4
G30.3	
G30.4	
G30.5	
G30.5	.5
G30.6	2
G30.7	.9
G30.8	3
G31.0	.8
G31.1	.0

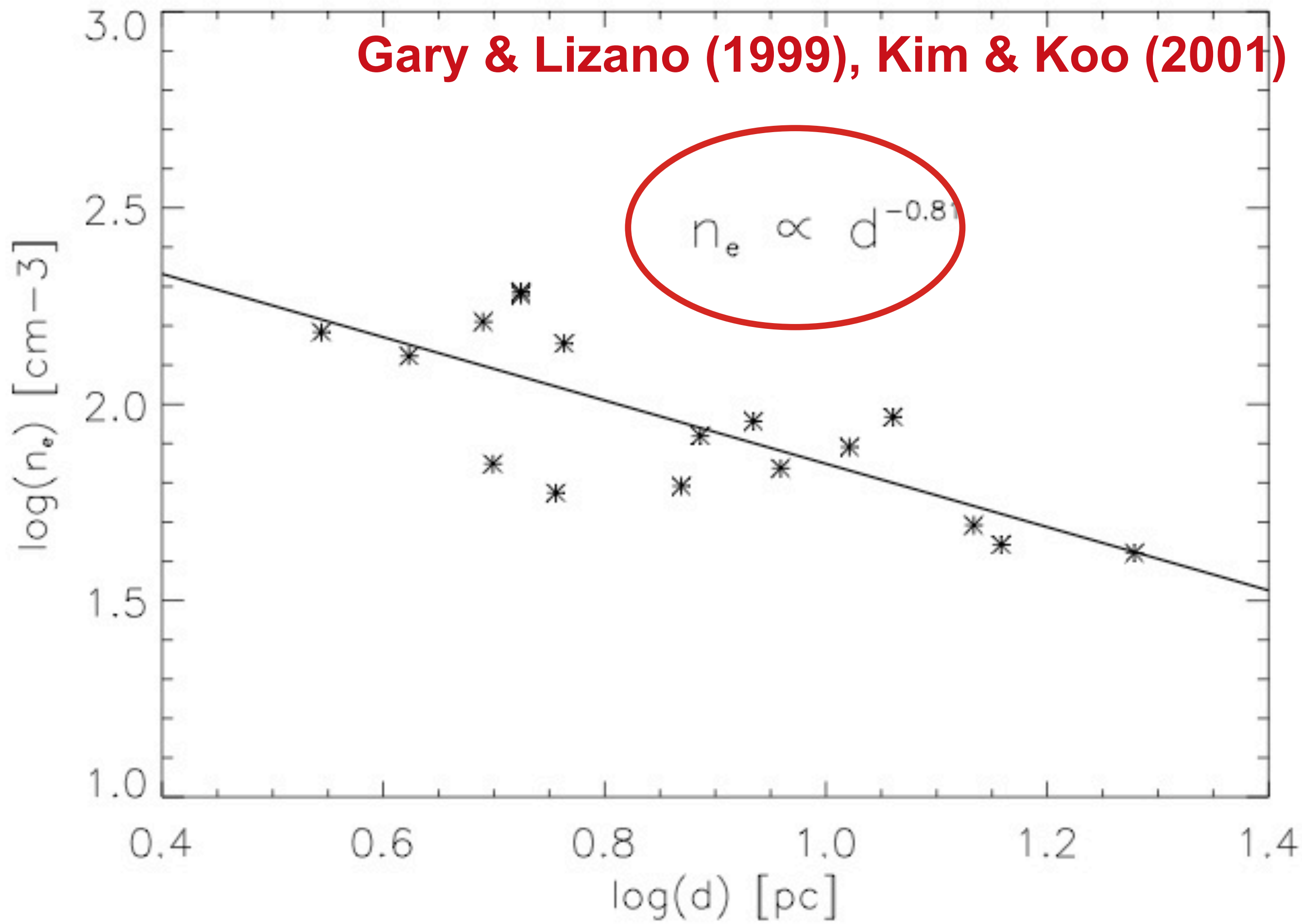

The use of ancillary high-resolution radio data:

2. Estimate of free-free contribution

- In order to build FIR/sub-mm SEDs, we need to subtract the free-free contribution at each wavelength.
- For an accurate evaluation of such a contribution, we use the MAGPIS 20-cm data, properly re-scaled at each PACS and SPIRE wavelength.
- For the re-scaling, we use:

$$\beta_{ff} = 2 + \frac{1}{10.48 + 1.5\ln(T_e/8000K) - \ln\nu_{GHz}}$$

(Bennett et al. 1992)

NOTE: between 70 and 500μm, β_{ff} varies, for the sources in our sample, in the range [-0.6, -0.2]. Hence, the subtraction of the free-free contribution becomes relevant only at at SPIRE 500μm. In general, though, we find that free-free emission is, at a given wavelength, orders of magnitudes (1 to 3) fainter than dust emission.

The use of ancillary high-resolution radio data:

2. Definition of photometric aperture

PACS 70μm > MAGPIS 20-cm

(13 sources)

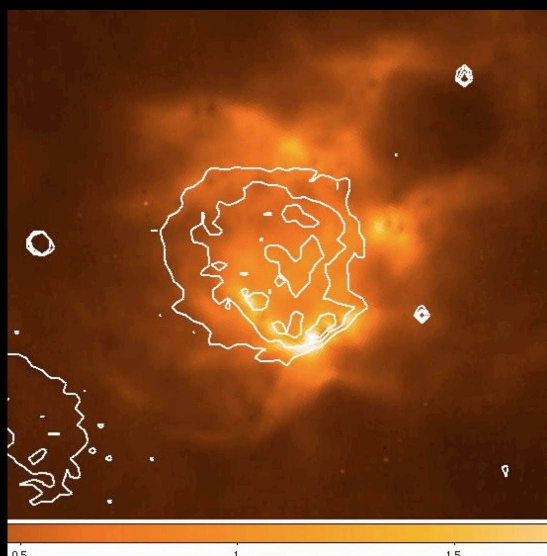

G29.0-0.6

PACS 70μm = MAGPIS 20-cm

(4 sources)

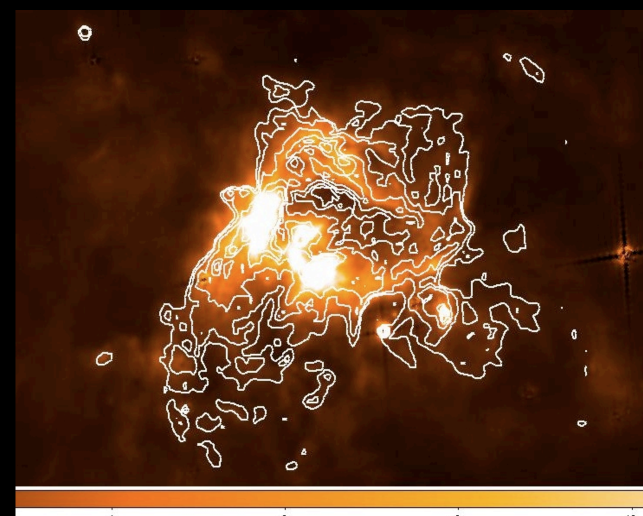

G30.8-0.0

Background image: PACS 70μm, contours: MAGPIS 20-cm data

BUILDING THE FIR/SUB-MM SEDs - I

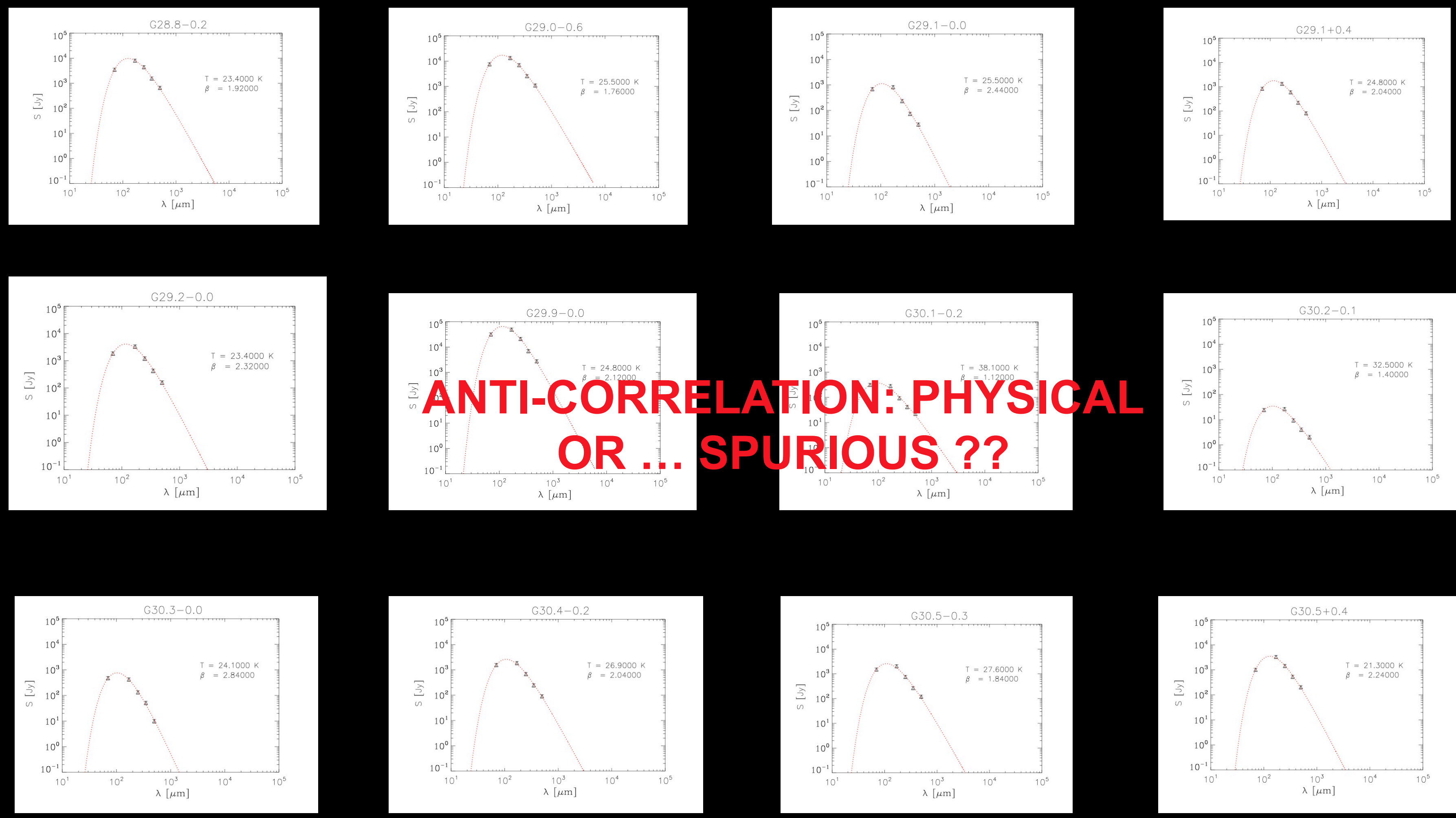

ANTI-CORRELATION: PHYSICAL OR … SPURIOUS ??

BUILDING THE FIR/SUB-MM SEDs - I

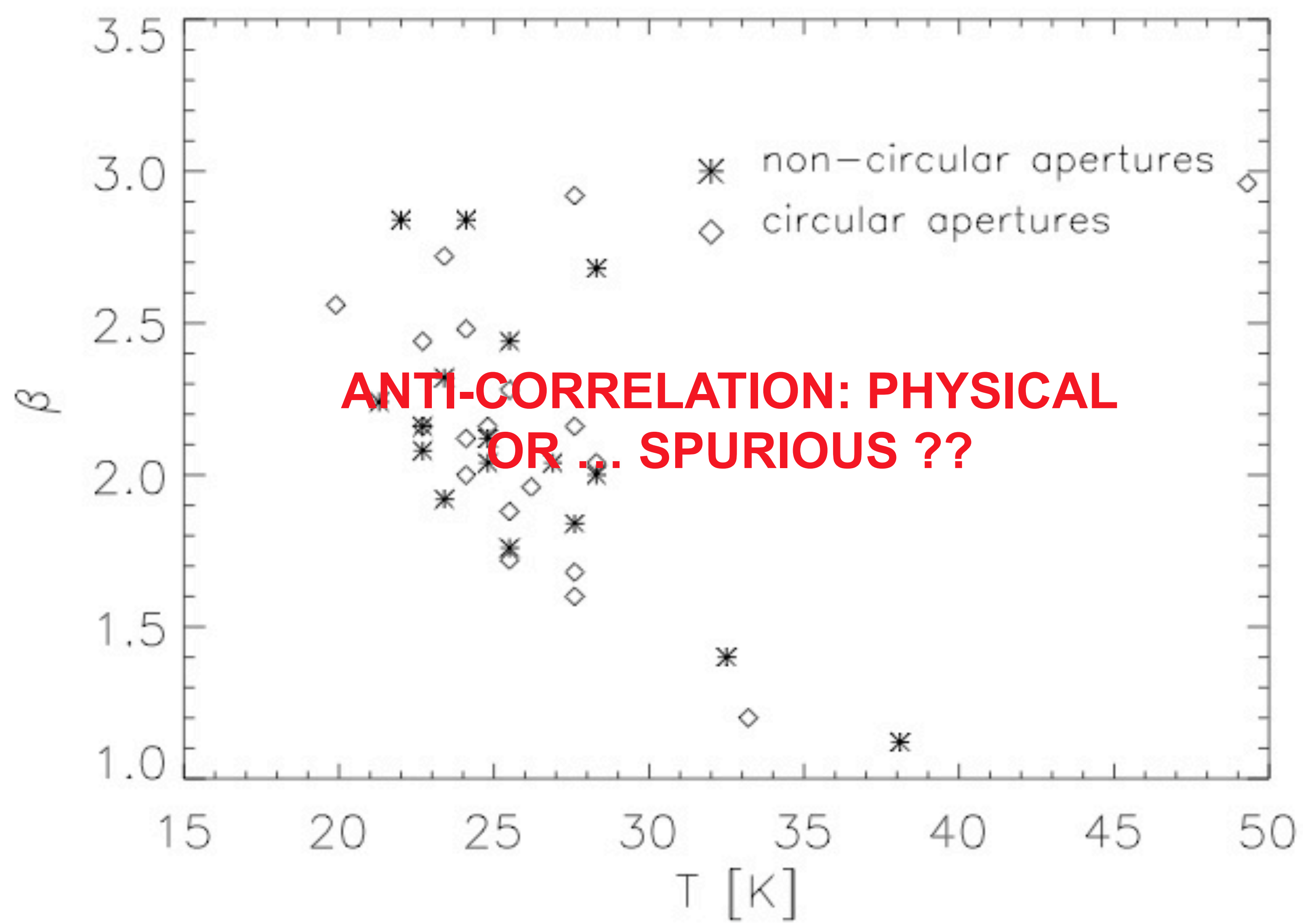

ANTI-CORRELATION: PHYSICAL OR … SPURIOUS ??

THE β - T RELATION

• At low temperatures, the sub-millimeter absorption in crystalline materials has a temperature-independent quadratic dependence on frequency. Such a temperature-independent quadratic dependence is also expected in amorphous solids (Boudet et al. 2005). Moreover, Big Grains (BGs) are mostly amorphous (Kemper et al. 2004). Thus, it is widely accepted that:

$$I_\upsilon = \varepsilon_{\nu_0} \left(\frac{\lambda}{\lambda_0} \right)^{-\beta} B_\upsilon(\lambda, T) \quad , \qquad \beta = 2$$

BUT

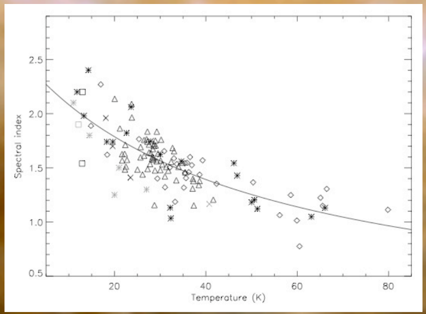

(Dupac et al. 2003)

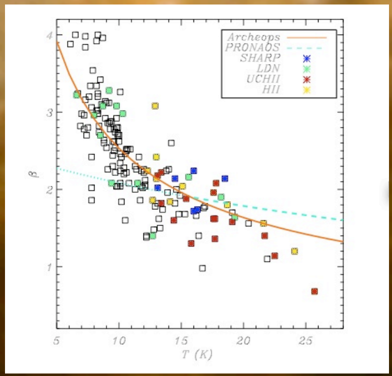

(Desert et al. 2008)

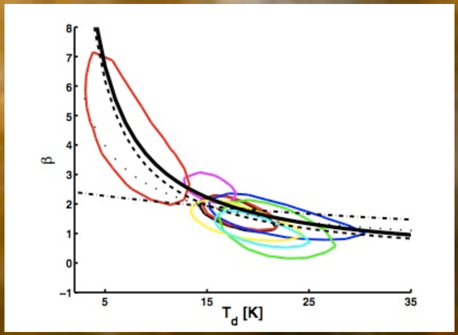

(Veneziani et al. 2010)

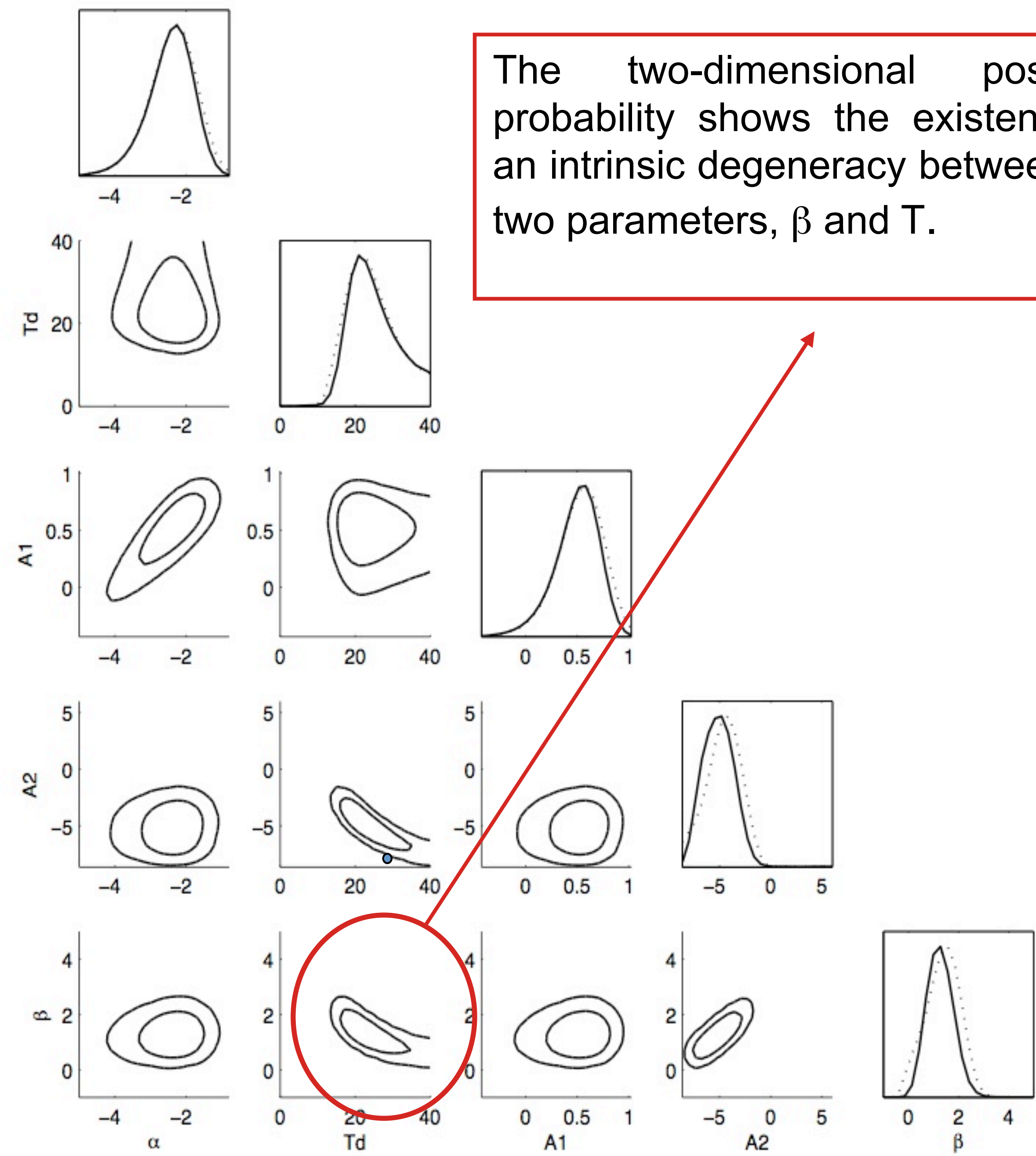

The two-dimensional posterior probability shows the existence of an intrinsic degeneracy between the two parameters, β and T.

Veneziani et al. 2010

BUILDING THE FIR/SUB-MM SEDs - II

To keep under control the degeneracy between the two parameters, we use a Monte Carlo Markov Chain (MCMC) algorithm (Christensen et al. 2001; Lewis & Bridle, 2002):

$$P(p \mid d) \propto P(p)P(d \mid p)$$

Posterior probability: $P(p \mid d)$

A priori probability: $P(p)$

Likelihood: $P(d \mid p)$

1) We first fit (using the MCMC), for each measured SEDs, the relation:

$$S \propto \upsilon^{\beta} B(\upsilon, T)$$

This operation allows also to build the confidence level contours for β and T in the parameters space.

2) then, we use again the MCMC technique to test the relation:

$$\beta = A \times T^{\gamma}$$

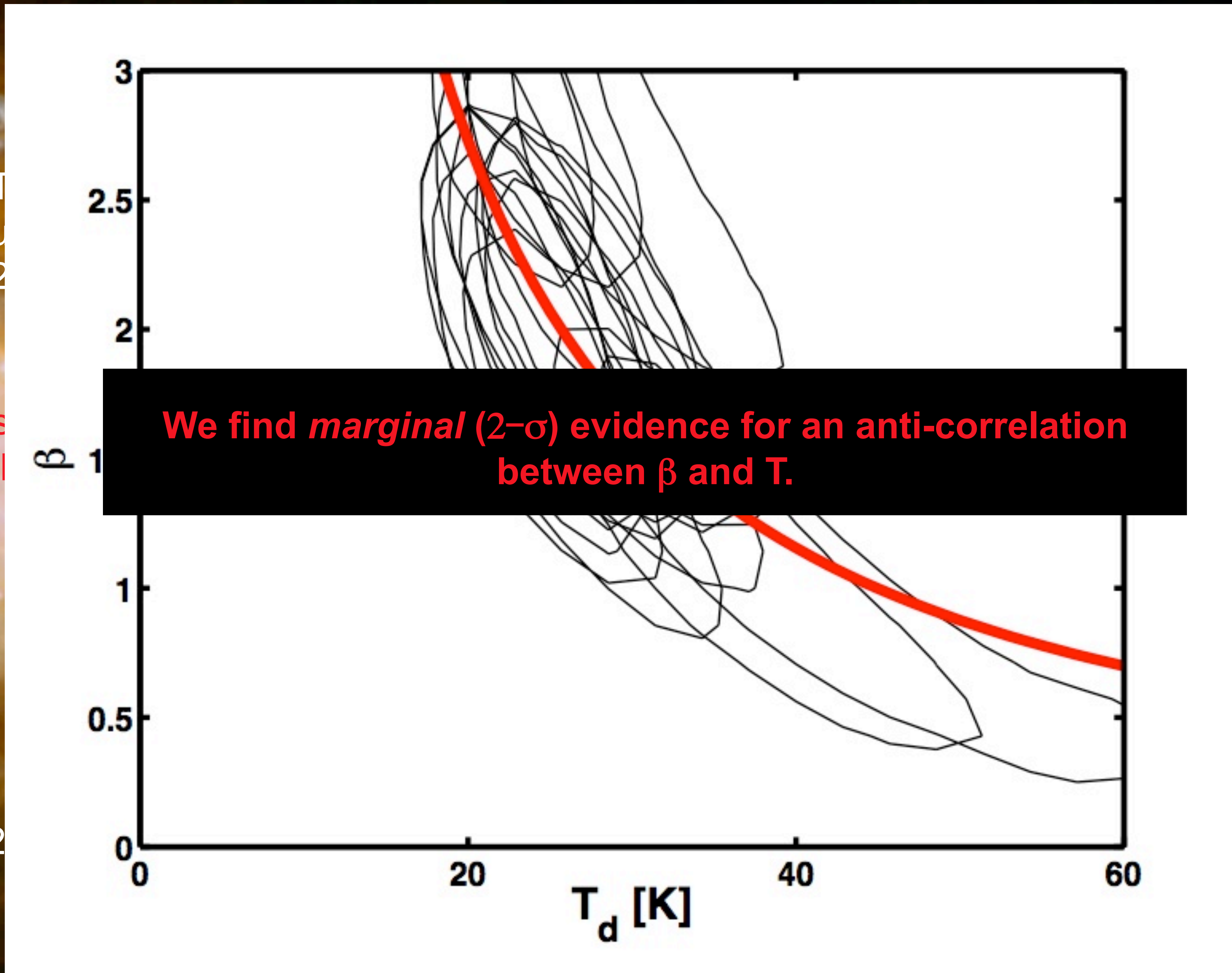

We find *marginal* (2−σ) evidence for an anti-correlation between β and T.

What are the FIR/sub-mm colors of these sources ?

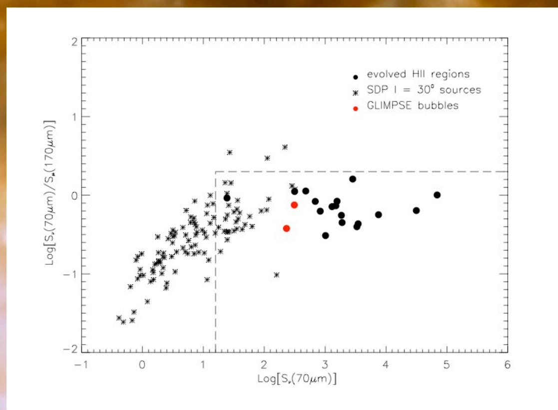

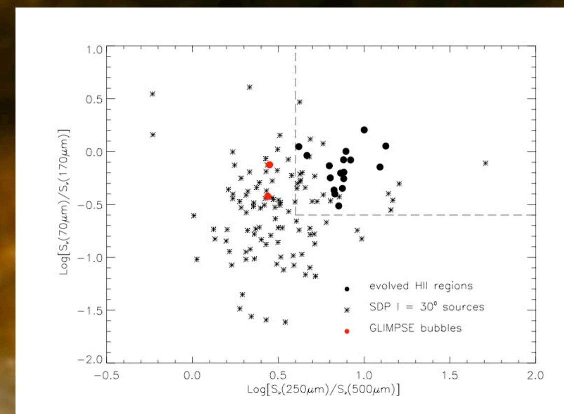

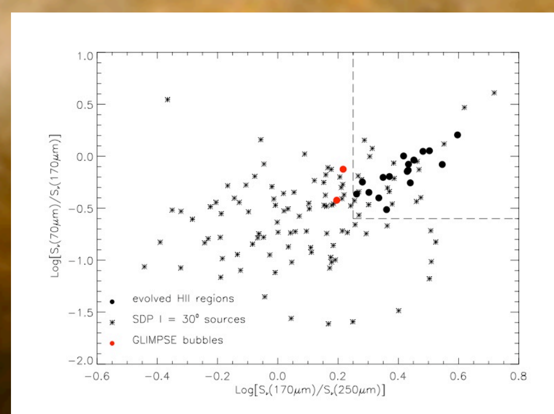

- ● HII regions
- + Elia et al. (2010)
- • Churchwell et al.

ESLAB 2010 - May 6th 2010

What are the FIR/sub-mm colors of these sources ?

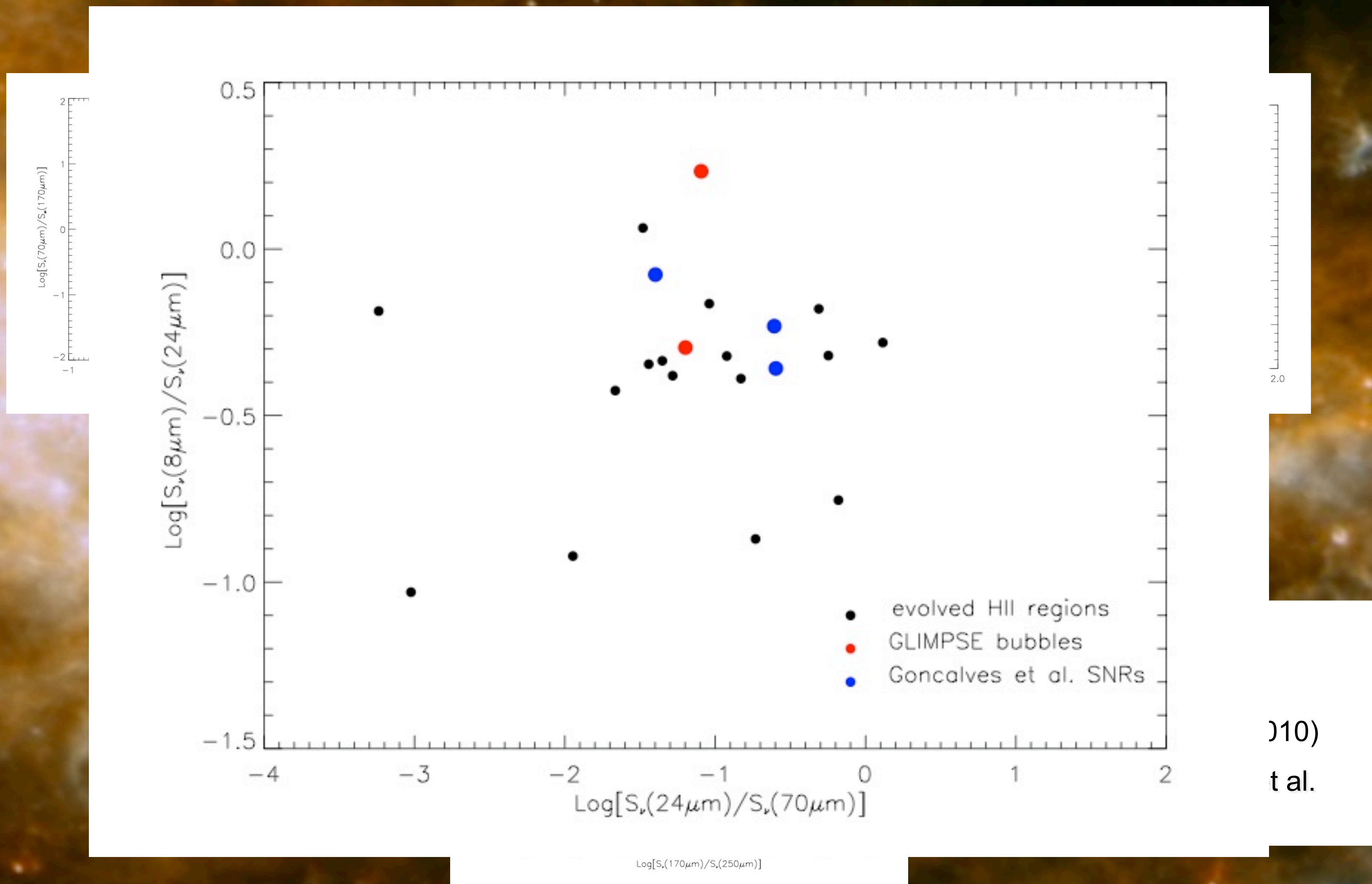

ESLAB 2010 - May 6th 2010

CONCLUSIONS

✓ We have studied a sample of 17 evolved HII regions in the Hi-GAL SDP field centered at l = 30^0

✓ The sample is well-defined and omogeneous

✓ From the ancillary single-dish radio data, we derive a n_e - d relation consistent with non-uniform sources (as expected)

✓ From the ancillary high-resolution radio data (MAGPIS), we obtain that the free-free contribution is mostly negligible at these wavelengths (it might be relevant only at 500μm and for a few sources)

✓ From the SED fits of the measured PACS/SPIRE fluxes, we obtained a temperature of dust in the range 20 - 40 K, and emissivity values in the range 1.1 to 3.

✓ we find marginal evidence (at a 2-σ) level, of an anti-correlation between β and T

✓ Evolved HII regions appear to have very well defined FIR and sub-mm colors with respect to other population of soures (GLIMPSE bubbles, etc)